HHS Public Access

Author manuscript

JACC Cardiovasc Imaging. Author manuscript; available in PMC 2023 April 01.

Published in final edited form as:

JACC Cardiovasc Imaging. 2022 April ; 15(4): 629–637. doi:10.1016/j.jcmg.2021.09.017.

Subclinical Pulmonary Congestion and Abnormal Hemodynamics in Heart Failure with Preserved Ejection Fraction

C. Charles Jain, MD[1], **Juerg Tschirren, PhD**[2], **Yogesh N.V. Reddy, MBBS**[1], **Vojtech Melenovsky, MD PhD**[3], **Margaret Redfield, MD**[1], **Barry A. Borlaug, MD**[1]

[1]Department of Cardiovascular Medicine, Mayo Clinic, Rochester, MN 55905

[2]Vida Diagnostics, 2500 Crosspark Rd., Suite W240, Coralville, IA 52241

[3]Institute for Clinical and Experimental Medicine (IKEM), Prague, 14021 Czech Republic

Abstract

Objectives: We hypothesized that quantitative computed tomography (QCT) would reveal subclinical increases in lung congestion in patients with heart failure and preserved ejection fraction (HFpEF) and that this would be related to pulmonary vascular hemodynamic abnormalities.

Background: Gross evidence of lung congestion on physical examination, laboratories, and radiography is typically absent among compensated ambulatory patients with HFpEF, yet pulmonary gas transfer abnormalities are commonly observed and associated with poor outcomes.

Methods: Patients referred for invasive hemodynamic exercise testing who had undergone chest computed tomography within 1 month were identified (n=137). A novel artificial intelligence QCT algorithm was used to measure pulmonary fluid content.

Results: As compared to controls with non-cardiac dyspnea, patients with HFpEF displayed increased mean lung density (−758 (−708, −194) vs. −787 (−828, −747) HU; p=0.002) and a higher ratio of extravascular lung water to total lung volume (EVLWV/TLV) (1.25 (0.80, 1.76) vs 0.66 (0.01, 1.03); p<0.0001) by QCT, indicating greater lung congestion. EVLWV/TLV was directly correlated with pulmonary vascular pressures at rest, with stronger correlations observed during exercise. Patients with increasing tertiles of EVLWV/TLV demonstrated higher mean pulmonary artery pressures at rest (34±11 vs 39±14 vs 45±17 mmHg; p=0.0003) and during exercise (55±17 vs 59±17 vs 69±22 mmHg; p=0.0003).

Conclusions: Quantitative CT identifies subclinical lung congestion in HFpEF that is not clinically apparent but is related to abnormalities in pulmonary vascular hemodynamics. These

Address for correspondence: Barry A. Borlaug, MD, Mayo Clinic and Foundation, 200 First Street SW, Rochester, MN 55905, Phone: 507-255-4152, Fax: 507-266-0228, borlaug.barry@mayo.edu.

Disclosures or Relations to Industry: Juerg Tschirren is the Director of Engineering at VIDA Diagnostics. There are no other relevant disclosures or relations to industry.

data provide new insight into the chronic effects of altered hemodynamics in HFpEF on pulmonary structure and function.

Keywords

heart failure; congestion; hemodynamics; exercise; computed tomography

Introduction

Pulmonary congestion is a hallmark of heart failure with preserved ejection fraction (HFpEF) that is associated with adverse outcomes.(1–6) Lung congestion in the early stages of HFpEF may be intermittent, developing only during acute hemodynamic insults such as exercise.(7) However, over time, repeated increases in pulmonary vascular pressures at rest and during exertion may cause subtle increases in extravascular lung water (EVLW), leading to alterations in gas exchange and pulmonary vascular remodeling.(8) These subclinical increases in EVLW are not typically apparent from standard clinical assessments such as physical examination or plain chest film,(9) but may lead to chronic alterations in gas exchange that are associated with exercise intolerance and increased mortality.(10,11)

Computed tomography (CT) distinguishes aerated lung, soft tissue and water content based upon radiographic attenuation characteristics with much greater precision and sensitivity, but this method is typically applied in only a qualitative way for clinical evaluation. (12–14) Recent advances in artificial intelligence (AI) enhanced quantitative CT (QCT) measurements may enable improved detection of even subclinical increases in EVLW. While AI-enabled QCT assessments have been applied to the evaluation of pulmonary diseases such as COVID-19 related pneumonia, there is little information available in patients with heart failure.(15,16)

We hypothesized that EVLW as measured by QCT would be increased at rest in HFpEF, even among well-compensated ambulatory patients, and that the magnitude of subclinical lung congestion would be related to resting and exercise induced pulmonary vascular hemodynamic abnormalities measured at cardiac catheterization.

Methods

Consecutive patients with unexplained dyspnea who underwent invasive cardiopulmonary exercise testing at the Mayo Clinic in Rochester, MN between March 2016 and June 2021 were retrospectively identified. HFpEF was defined according to current guidelines as patients with exertional dyspnea, EF≥50%, with pulmonary capillary wedge pressure (PCWP) at rest ≥15 mmHg or with exercise ≥25 mmHg, and no alternative cause of symptoms.(17,18) Control patients with non-cardiac etiologies of dyspnea were defined as those with resting PCWP <15 mmHg and mean pulmonary artery (PA) pressure <25 mmHg, and exercise PCWP <25 mmHg and exercise mean PA pressure <35 mmHg. Patients with left ventricular ejection fraction <50%, significant pulmonary parenchymal disease, primary right-sided heart failure, valvular heart disease (>moderate left-sided regurgitation and/or >mild stenosis), unstable coronary disease, high-output heart failure, constrictive pericarditis, and infiltrative, restrictive, or hypertrophic cardiomyopathy were

excluded. Transthoracic echocardiography was performed prior to catheterization according to guideline recommendations.(19,20) The Institutional Review Board approved the study.

Quantitative Computed Tomography

Patients who had undergone chest CT as part of their clinical evaluation within 1 month of cardiac catheterization were included. The types of CT studies included non-contrast studies protocoled to evaluate lung fields, non-contrast studies for coronary calcium assessment, contrast studies dedicated for cardiac and angiographic evaluation, or contrast studies not otherwise specified. When the study was ordered with contrast, the pre-contrast images were used. The only type of CT study not included was positron emission tomography. All scans were performed using either a Siemens or GE machine. Imaging was performed during a breath hold at inspiration.

Quantitative CT analysis was performed in a blinded fashion from de-identified images by VIDA Diagnostics (Coralville, IA), using a novel proprietary algorithm based upon Hounsfield units (HU) and anatomic assessment for vascular tree structures. This artificial intelligence (AI) software has previously been validated in large populations of patients with chronic pulmonary diseases, including assessment of the vascular contributions to lung disease.(21–24) Briefly, digital masks of whole lung, individual lungs, and pulmonary vascular tree were segmented from CT images. Any blood vessels readily identifiable on CT, adjacent tissues, and pleural space were excluded. Volumes were measured in arbitrary units (AU) where each voxel represents 1 AU.

Voxels falling within the attenuation range of air (−1000 HU) and water (0 HU) were included in the analysis. Most voxels fall between these extremes as they contain a combination of air and water, but as fluid content increases, more voxels move toward 0 HU, becoming less negative. Mean lung density (MLD) was calculated from the attenuation distribution within the segmented areas. Lung fluid was quantified as fluid content (FC) from the measured MLD as FC = (MLD+1000)/10.(25) The distribution of voxels in the lung is characterized by the MLD, skew and kurtosis. As EVLW increases, the MLD increases (rightward shift in the histogram) and the skew and kurtosis decrease (curve becomes wider and shorter).(14,26)

From the lung masks, total lung volume (TLV) was divided into tissue volume and air volume compartments. The tissue volume was further divided into vessel volume, water volume, blood volume, and other components depending on voxel density and reported in AU. Blood volume was defined as all voxels in the (13, 50) HU range, while water volume included all voxels in the (−10, 10) HU range. Extravascular lung water volume (EVLWV) was defined as the total water volume in the lungs excluding identifiable vessels. EVLWV was then indexed to TLV for the primary analysis (EVLWV/TLV).

Invasive Hemodynamic Assessment

Patients were evaluated in the fasted state on chronic medications with minimal sedation and in the supine position, as previously described.(27–29) Right heart catheterizations were performed via the right internal jugular vein at rest and with exercise. Simultaneous direct measurements of oxygen consumption (VO_2) were made using expired gas analysis

(MedGraphic St. Paul, MN, USA). Blood gas analysis was performed on arterial and pulmonary arterial samples to calculate arteriovenous oxygen difference (AVO_2diff). Cardiac output was assessed by direct Fick method (CO = VO_2/AVO_2diff). Right atrial, PA pressures, and PCWP were measured at end-expiration as the mean of ≥3 beats. Pulmonary artery compliance was calculated using [(stroke volume) / (systolic PA pressure − diastolic PA pressure)]. Pulmonary artery elastance was calculated using (systolic PA pressure) / (stroke volume).

Following resting measurements, patients performed supine cycle ergometry starting at a workload of 20 W for 5 minutes, increasing by 20 W (3 min per stage) until subject-reported exhaustion. The same methods for blood gas analysis and hemodynamic data were again used for measurements at peak exercise.

Statistical Analysis

Data are reported as mean ± standard deviation, median (25^{th}, 75^{th} percentile), or numbers (percentages). Data are reported as mean ± standard deviation, median (25^{th}, 75^{th} percentile), or numbers (percentages). For variables with a Gaussian distribution, group comparisons were made using one-way analysis of variance (ANOVA), while non-normally distributed data were analyzed using the Kruskal-Wallis test. Categorical variables were compared using the Chisquare test. Simple linear regression was used to assess correlations between EVLWV/TLV (log transformed) and hemodynamics. Multivariable linear regression was used to adjust for age, sex, and BMI. Logistic regression was used to describe predictive ability of QCT parameters for HFpEF and to identify optimal cutoffs based on the area under the receiver operator curve (AUC). Patients were divided into tertiles of EVLWV/TLV. Sensitivity analysis using a cohort of patients who had CT within 6 months of catheterization was performed, using frequency matching to achieve comparable ages and weights between cases and controls. All p values are two-sided with predefined significance level of <0.05. Analyses performed using JMP 14.1 (SAS Institute, Cary, NC, USA).

Results

As compared to controls (n=38), patients with HFpEF (n=99) were older and had higher body mass index (BMI), greater comorbidity burden, were more likely to be treated with diuretics and neurohormonal antagonists, and had higher NT-proBNP levels (Table 1). Patients with HFpEF displayed greater left ventricular mass, abnormal diastolic function, and elevated estimated right ventricular systolic pressure, along with higher right and left heart filling pressures and pulmonary artery pressures as compared to controls.

The interval between CT and hemodynamic evaluation was −2 (−1, −7) days. Patients with HFpEF displayed greater lung congestion, evidenced by higher MLD (−787 (−828, −747 vs −758 (−194, −708) HU, p=0.002), along with lower skew and kurtosis (Table 2, Central Illustration). Total lung volume was not significantly different between HFpEF and controls. Patients with HFpEF displayed similar vessel volume, but higher blood volume (8.5 (5.13, 12.4) vs 5.2 (2.98, 7.41) AU, p=0.0003), extravascular lung water volume (5.2 (2.9, 7.8) vs 2.7 (1.5, 4.3) AU, p<0.0001) and EVLWV/TLV ratio (1.25 (0.80, 1.76) vs 0.66 (0.01, 1.03) AU/l, p<0.0001, Table 2, Central Illustration).

The area under the curve (AUC) of the receiver operating characteristic curve of EVLWV/TLV to discriminate HFpEF from controls was 0.74, with an optimal cutoff value of 1.05 (sensitivity of 63%, specificity of 78%, positive likelihood ratio 2.9, negative likelihood ratio 0.5). Differences in EVLWV/TLV ratio between HFpEF and control groups remained significant after adjusting for age, sex, and BMI ($p<0.05$) on multivariable linear regression analysis. In a second sensitivity analysis where cases and controls were frequency matched for age and BMI, there were again significant differences in EVLWV/TLV ratio between HFpEF and controls (Supplemental Table 1).

There were modest positive correlations between EVLWV/TLV and echocardiographic Doppler mitral inflow E velocities and E/e' (Supplemental Table 2). There was also a direct correlation between EVLWV/TLV and resting PCWP and PA pressures (Table 3, Figure 1). Interestingly, even as CT had been performed at rest, the correlation between EVLWV/TLV and mean PA pressures became stronger during exercise ($r=0.53$, $p<0.0001$; Table 3, Figure 1). Left and right heart filling pressures were also directly related to EVLWV/TLV, with stronger associations during exercise, similar to relationships with PA pressures. There was a modest inverse correlation between EVLWV/TLV and peak VO_2 ($r= -0.33$, $p<0.001$). Findings were similar in the subset of patients who had CT performed within 1 week of catheterization (Supplemental Table 2). Pulmonary artery systolic pressure increased with increasing tertiles of EVLWV/TLV, both at rest (34±11 vs 39±14 vs 45±17 mmHg; $p=0.003$) and during exercise (55±17 vs 59±17 vs 69±22 mmHg; $p=0.003$) (Figure 2).

Discussion

Despite the absence of clinically overt congestion, we found that patients with HFpEF display increased EVLW by QCT as compared to controls with non-cardiac etiologies of dyspnea. The amount of EVLW was correlated with abnormal pulmonary vascular hemodynamics at rest, and correlations became stronger during exercise, even as CT imaging was performed remotely from the time of cardiac catheterization and at rest. These findings demonstrate that lung congestion is present even among apparently well-compensated ambulatory patients with HFpEF, including patients with normal or near-normal hemodynamics measured at rest.

Nearly 40 years ago the potential value of QCT was suggested by the demonstration that lung density is dynamic and can acutely increase in the setting of pulmonary edema.(12,30) Lung density by QCT has subsequently been correlated with lung water as measured invasively using the thermal indocyanine green-dye double dilution technique in patients with pulmonary edema due to acute respiratory distress syndrome.(31) In patients with heart failure with reduced ejection fraction, conventional CT imaging has been used to measure mean lung density to estimate lung water content, showing that lung density and estimated fluid content are greater among patients with active heart failure decompensation.(25) Ambulatory patients with HFpEF typically do not display physical exam or radiographic evidence of lung congestion, but studies evaluating pulmonary capillary gas diffusion have consistently identified impairments in HFpEF at rest and during exercise, which are strongly related to increased risk of death.(10,11) The causes of these abnormalities are suspected to

be related to long term exposure to left atrial hypertension, but few studies have evaluated this possibility.

To the best of our knowledge, this is the first study to evaluate lung congestion in ambulatory patients with HFpEF using QCT, and the first to perform correlations with invasive hemodynamics at rest and exercise. Increases in EVLWV/TLV were modestly correlated with PCWP, with greater correlation to exercise values. However, PCWP elevation is not the only important factor in development of EVLW.(1,7,8) Elevations in central venous pressure due to right-sided heart failure may impair pulmonary lymphatic drainage,(7) and it is important to remember that PCWP is an underestimate of the true pressure driving EVLW accumulation, known as pulmonary capillary pressure (P_{cap}). (8) P_{cap} increases relative to PCWP as pulmonary venous resistance increases, which may occur with more severe pulmonary hypertension and venous remodeling in HFpEF. (8,32,33) We observed that pulmonary vascular resistance during exercise was also related to EVLWV/TLV. This is typically conceptualized as a measure reflecting pulmonary arteriolar pathologies, but elevations in pulmonary venous resistance may also contribute.(8)

Interestingly, hemodynamics with exercise displayed stronger correlations with QCT measurements of EVLW than corresponding values at rest. This raises an interesting hypothesis that repeated exposures to low-level hemodynamic stress during activities of daily living may lead to accumulation of subclinical increases in EVLW. We also found a modest inverse correlation between EVLWV/TLV and aerobic capacity (peak VO_2), supporting the hypothesis that increases in lung congestion relate to functional limitation in HFpEF. Pulmonary vascular remodeling is common in HFpEF, even as pressures may be normal at rest.(33) With stress, patients with HFpEF have been shown to have significant alteration in right heart function and pulmonary vascular hemodynamics.(27,34,35) This repetitive strain on the pulmonary vascular bed can further exacerbate reactive pulmonary hypertension and impair pulmonary capillary function by causing stress fracture in the capillary bed. The lungs represent the most direct victim of left heart disease in patients with left-sided heart failure, and patients with more lung congestion or long-term sequelae of congestion might merit consideration as a distinct phenotype that requires novel treatments, some of which are already under investigation.(36–38) The present data suggest that QCT could have a potential role in clinical assessment of lung congestion in patients with HFpEF, though further studies are needed for external validation of this novel method and refinement of the AI algorithm.

Advantages of AI for QCT analysis include the fact that the algorithm is set within the software, with fully automated image interpretation. There are no manual edits performed or human interpretation, so there is no intraobserver or interobserver variability, allowing for robust reproducibility. The analysis can be performed on any standard computer with a duration of 60–90 seconds per scan.

Limitations

This study is limited by its retrospective, cross sectional nature. By design, only patients referred for chest CT could be included. While the impact of this bias is reduced through use of strict eligibility criteria and exclusion of patients with lung disease, referral bias

remains a limitation. CTs were collected within one month of catheterization, and while this could impact correlations between the two studies, sensitivity analyses restricted to patients undergoing CT within 1 week of catheterization did not show any significant differences. The control group was not truly normal as they had symptoms of dyspnea prompting evaluation, but this would only be expected to bias our results toward the null. The HFpEF group was older and had higher BMI, however, matched analysis and multivariable analysis showed the differences in CT findings were significant despite these potential confounders. We describe use of a novel AI algorithm that has yet to be established in other populations and does not have widespread availability, and further validation studies will be required prior to adoption into clinical practice.

Conclusion

Ambulatory patients with HFpEF display increased lung congestion that is not apparent from conventional clinical indicators when evaluated using quantitative chest CT imaging. These low-grade increases in EVLW are correlated with abnormalities in resting and exercise pulmonary vascular pressures, suggesting a new hypothesis that chronic repeated exposure to elevations in pulmonary pressure may drive chronic lung congestion and its secondary effects on gas transfer and pulmonary vascular properties. Further study is required to define the role for QCT in the evaluation and care of patients with HFpEF and to better delineate the pathophysiologic determinants and clinical relevance of these subclinical increases in lung congestion identified by QCT.

Supplementary Material

Refer to Web version on PubMed Central for supplementary material.

Financial Support:

Dr. Borlaug is supported by R01 HL128526.

Abbreviations List

AI	artificial intelligence
AU	arbitrary units
AUC	area under the curve
CT	computed tomography
EVLW	extravascular lung water
EVLWV	extravascular lung water volume
EVLWV/TLV	extravascular lung water volume indexed to total lung volume
HFpEF	heart failure with preserved ejection fraction
P_{cap}	pulmonary capillary pressure

PCWP	pulmonary capillary wedge pressure
QCT	quantitative computed tomography
TLV	total lung volume
VO_2	oxygen consumption

References

1. Melenovsky V, Andersen MJ, Andress K, Reddy YN, Borlaug BA. Lung congestion in chronic heart failure: haemodynamic, clinical, and prognostic implications. Eur J Heart Fail 2015;17:1161–71. [PubMed: 26467180]
2. Platz E, Merz AA, Jhund PS, Vazir A, Campbell R, McMurray JJ. Dynamic changes and prognostic value of pulmonary congestion by lung ultrasound in acute and chronic heart failure: a systematic review. Eur J Heart Fail 2017;19:1154–1163. [PubMed: 28557302]
3. Selvaraj S, Claggett B, Pozzi A et al. Prognostic Implications of Congestion on Physical Examination Among Contemporary Patients With Heart Failure and Reduced Ejection Fraction: PARADIGM-HF. Circulation 2019;140:1369–1379. [PubMed: 31510768]
4. Koell B, Zotter-Tufaro C, Duca F et al. Fluid status and outcome in patients with heart failure and preserved ejection fraction. International journal of cardiology 2017;230:476–481. [PubMed: 28062131]
5. Zile MR, Bennett TD, El Hajj S et al. Intracardiac Pressures Measured Using an Implantable Hemodynamic Monitor: Relationship to Mortality in Patients With Chronic Heart Failure. Circ Heart Fail 2017;10.
6. Kociol RD, McNulty SE, Hernandez AF et al. Markers of decongestion, dyspnea relief, and clinical outcomes among patients hospitalized with acute heart failure. Circ Heart Fail 2013;6:240–5. [PubMed: 23250981]
7. Reddy YNV, Obokata M, Wiley B et al. The haemodynamic basis of lung congestion during exercise in heart failure with preserved ejection fraction. Eur Heart J 2019;40:3721–3730. [PubMed: 31609443]
8. Verbrugge FH, Guazzi M, Testani JM, Borlaug BA. Altered Hemodynamics and EndOrgan Damage in Heart Failure: Impact on the Lung and Kidney. Circulation 2020;142:998–1012. [PubMed: 32897746]
9. Stevenson LW, Perloff JK. The limited reliability of physical signs for estimating hemodynamics in chronic heart failure. JAMA 1989;261:884–8. [PubMed: 2913385]
10. Olson TP, Johnson BD, Borlaug BA. Impaired Pulmonary Diffusion in Heart Failure With Preserved Ejection Fraction. JACC Heart Fail 2016;4:490–8. [PubMed: 27256752]
11. Hoeper MM, Meyer K, Rademacher J, Fuge J, Welte T, Olsson KM. Diffusion Capacity and Mortality in Patients With Pulmonary Hypertension Due to Heart Failure With Preserved Ejection Fraction. JACC Heart Fail 2016;4:441–9. [PubMed: 26874383]
12. Morooka N, Watanabe S, Masuda Y, Inagaki Y. Estimation of pulmonary water distribution and pulmonary congestion by computed tomography. Jpn Heart J 1982;23:697–709. [PubMed: 7176078]
13. Jorgenson CC, Chase SC, Olson LJ, Johnson BD. Assessment of Thoracic Blood Volume by Computerized Tomography in Patients With Heart Failure and Periodic Breathing. J Card Fail 2018;24:479–483. [PubMed: 29678727]
14. Chase SC, Taylor BJ, Cross TJ, Coffman KE, Olson LJ, Johnson BD. Influence of Thoracic Fluid Compartments on Pulmonary Congestion in Chronic Heart Failure. J Card Fail 2017;23:690–696. [PubMed: 28716688]
15. Nagpal P, Narayanasamy S, Vidholia A et al. Imaging of COVID-19 pneumonia: Patterns, pathogenesis, and advances. Br J Radiol 2020;93:20200538. [PubMed: 32758014]
16. Newell JD Jr., Tschirren J, Peterson S, Beinlich M, Sieren J. Quantitative CT of Interstitial Lung Disease. Semin Roentgenol 2019;54:73–79. [PubMed: 30685002]

17. Borlaug BA. Evaluation and management of heart failure with preserved ejection fraction. Nature reviews Cardiology 2020;17:559–573. [PubMed: 32231333]

18. Pieske B, Tschope C, de Boer RA et al. How to diagnose heart failure with preserved ejection fraction: the HFA-PEFF diagnostic algorithm: a consensus recommendation from the Heart Failure Association (HFA) of the European Society of Cardiology (ESC). Eur Heart J 2019;40:3297–3317. [PubMed: 31504452]

19. Lang RM, Badano LP, Mor-Avi V et al. Recommendations for cardiac chamber quantification by echocardiography in adults: an update from the American Society of Echocardiography and the European Association of Cardiovascular Imaging. J Am Soc Echocardiogr 2015;28:1–39 e14. [PubMed: 25559473]

20. Nagueh SF, Smiseth OA, Appleton CP et al. Recommendations for the Evaluation of Left Ventricular Diastolic Function by Echocardiography: An Update from the American Society of Echocardiography and the European Association of Cardiovascular Imaging. J Am Soc Echocardiogr 2016;29:277–314. [PubMed: 27037982]

21. Coxson HO, Leipsic J, Parraga G, Sin DD. Using pulmonary imaging to move chronic obstructive pulmonary disease beyond FEV1. Am J Respir Crit Care Med 2014;190:135–44. [PubMed: 24873985]

22. Woodruff PG, Barr RG, Bleecker E et al. Clinical Significance of Symptoms in Smokers with Preserved Pulmonary Function. The New England journal of medicine 2016;374:1811–21. [PubMed: 27168432]

23. Sieren JP, Newell JD Jr., Barr RG et al. SPIROMICS Protocol for Multicenter Quantitative Computed Tomography to Phenotype the Lungs. Am J Respir Crit Care Med 2016;194:794–806. [PubMed: 27482984]

24. Iyer KS, Newell JD Jr., Jin D et al. Quantitative Dual-Energy Computed Tomography Supports a Vascular Etiology of Smoking-induced Inflammatory Lung Disease. Am J Respir Crit Care Med 2016;193:652–61. [PubMed: 26569033]

25. Amir O, Azzam ZS, Gaspar T et al. Validation of remote dielectric sensing (ReDS) technology for quantification of lung fluid status: Comparison to high resolution chest computed tomography in patients with and without acute heart failure. International journal of cardiology 2016;221:841–6. [PubMed: 27434357]

26. Kato S, Nakamoto T, Iizuka M. Early diagnosis and estimation of pulmonary congestion and edema in patients with left-sided heart diseases from histogram of pulmonary CT number. Chest 1996;109:1439–45. [PubMed: 8769490]

27. Gorter TM, Obokata M, Reddy YNV, Melenovsky V, Borlaug BA. Exercise unmasks distinct pathophysiologic features in heart failure with preserved ejection fraction and pulmonary vascular disease. Eur Heart J 2018;39:2825–2835. [PubMed: 29947750]

28. Reddy YNV, Olson TP, Obokata M, Melenovsky V, Borlaug BA. Hemodynamic Correlates and Diagnostic Role of Cardiopulmonary Exercise Testing in Heart Failure With Preserved Ejection Fraction. JACC Heart Fail 2018;6:665–675. [PubMed: 29803552]

29. Obokata M, Kane GC, Reddy YN, Olson TP, Melenovsky V, Borlaug BA. Role of Diastolic Stress Testing in the Evaluation for Heart Failure With Preserved Ejection Fraction: A Simultaneous Invasive-Echocardiographic Study. Circulation 2017;135:825–838. [PubMed: 28039229]

30. Kalef-Ezra J, Karantanas A, Tsekeris P. CT measurement of lung density. Acta Radiol 1999;40:333–7. [PubMed: 10335975]

31. Patroniti N, Bellani G, Maggioni E, Manfio A, Marcora B, Pesenti A. Measurement of pulmonary edema in patients with acute respiratory distress syndrome. Crit Care Med 2005;33:2547–54. [PubMed: 16276179]

32. Ganter CC, Jakob SM, Takala J. Pulmonary capillary pressure. A review. Minerva Anestesiol 2006;72:21–36. [PubMed: 16407804]

33. Fayyaz AU, Edwards WD, Maleszewski JJ et al. Global Pulmonary Vascular Remodeling in Pulmonary Hypertension Associated with Heart Failure and Preserved or Reduced Ejection Fraction. Circulation 2018;137:1796–1810. [PubMed: 29246894]

34. Andersen MJ, Hwang SJ, Kane GC et al. Enhanced pulmonary vasodilator reserve and abnormal right ventricular: pulmonary artery coupling in heart failure with preserved ejection fraction. Circ Heart Fail 2015;8:542–50. [PubMed: 25857307]

35. Borlaug BA, Kane GC, Melenovsky V, Olson TP. Abnormal right ventricular-pulmonary artery coupling with exercise in heart failure with preserved ejection fraction. Eur Heart J 2016;37:3293–3302.

36. Reddy YNV, Obokata M, Koepp KE, Egbe AC, Wiley B, Borlaug BA. The beta-Adrenergic Agonist Albuterol Improves Pulmonary Vascular Reserve in Heart Failure With Preserved Ejection Fraction. Circ Res 2019;124:306–314. [PubMed: 30582447]

37. Taylor BJ, Snyder EM, Richert ML et al. Effect of beta2-adrenergic receptor stimulation on lung fluid in stable heart failure patients. J Heart Lung Transplant 2017;36:418–426. [PubMed: 27863863]

38. Stewart GM, Johnson BD, Sprecher DL et al. Targeting pulmonary capillary permeability to reduce lung congestion in heart failure: a randomized, controlled pilot trial. Eur J Heart Fail 2020;22:1641–1645.. [PubMed: 32227554]

Clinical Perspectives

Competencies in Medical Knowledge

We demonstrate that subclinical lung congestion is commonly present among stable ambulatory patients, and by correlating this with invasive exercise hemodynamics, this study provides new insight to the mechanisms in which patients with heart failure develop pulmonary abnormalities even when clinically appearing euvolemic.

Translational Outlook

Artificial intelligence-enabled quantitative computed tomography analysis is a novel assessment of lung congestion in heart failure and more studies are needed to characterize and refine the capabilities of this technology to clarify its potential role in future research and clinical assessment of patients with heart failure.

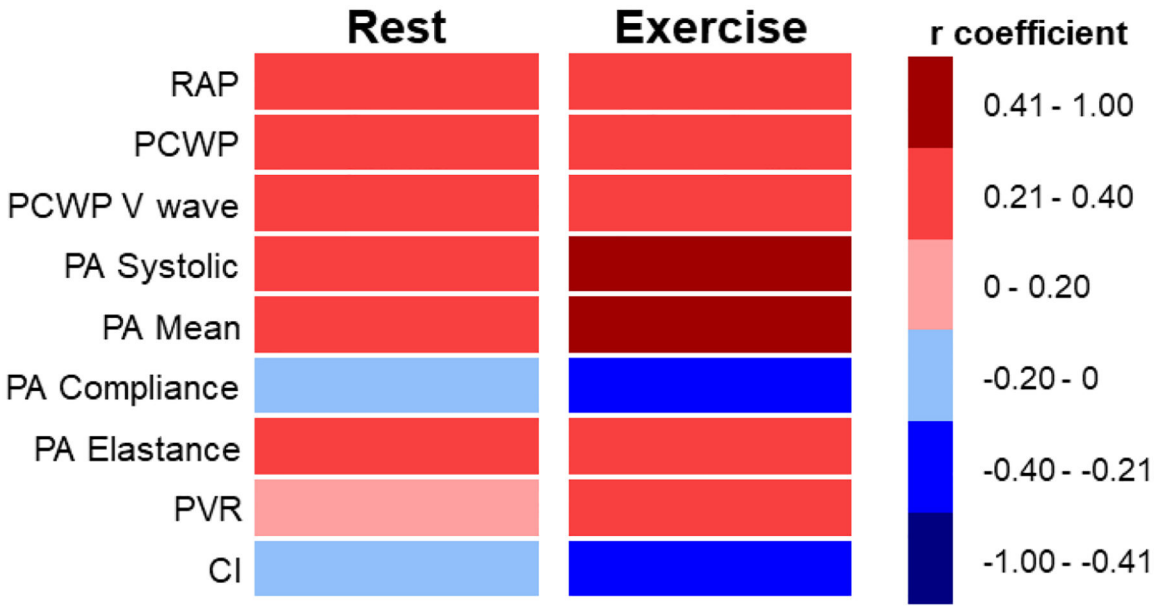

Figure 1: Correlations between Lung Congestion and Invasive Hemodynamics

Heat map displaying correlations between extravascular lung water (Log [EVLWV/TLV]) with invasive hemodynamic measures. The left column displays correlation for all patients at rest and the right column displays correlations for all patients at peak exercise.

Abbreviations: EVLWV/TLV = extravascular lung water volume indexed to total lung volume; PA = pulmonary artery; PCWP = pulmonary capillary wedge pressure; PVR = pulmonary vascular resistance; RAP = right atrial pressure

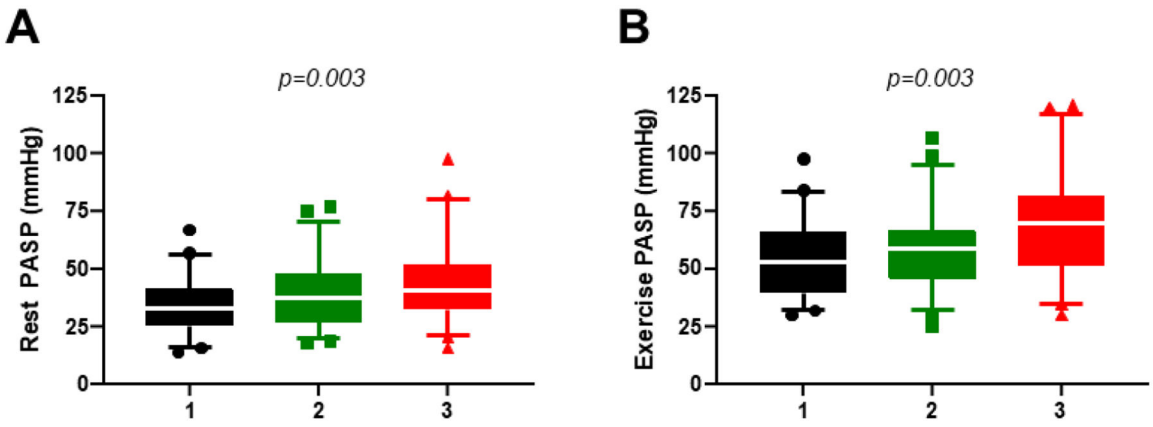

Figure 2: Pulmonary Artery Pressures at Rest and Exercise and Lung Water

Pulmonary artery systolic pressure (PASP) measured at catheterization increased from patients in the lowest tertile of extravascular lung water volume indexed to total lung volume (black) to the middle (green) and highest tertile (red) at rest (left panels) and during exercise (right panels).

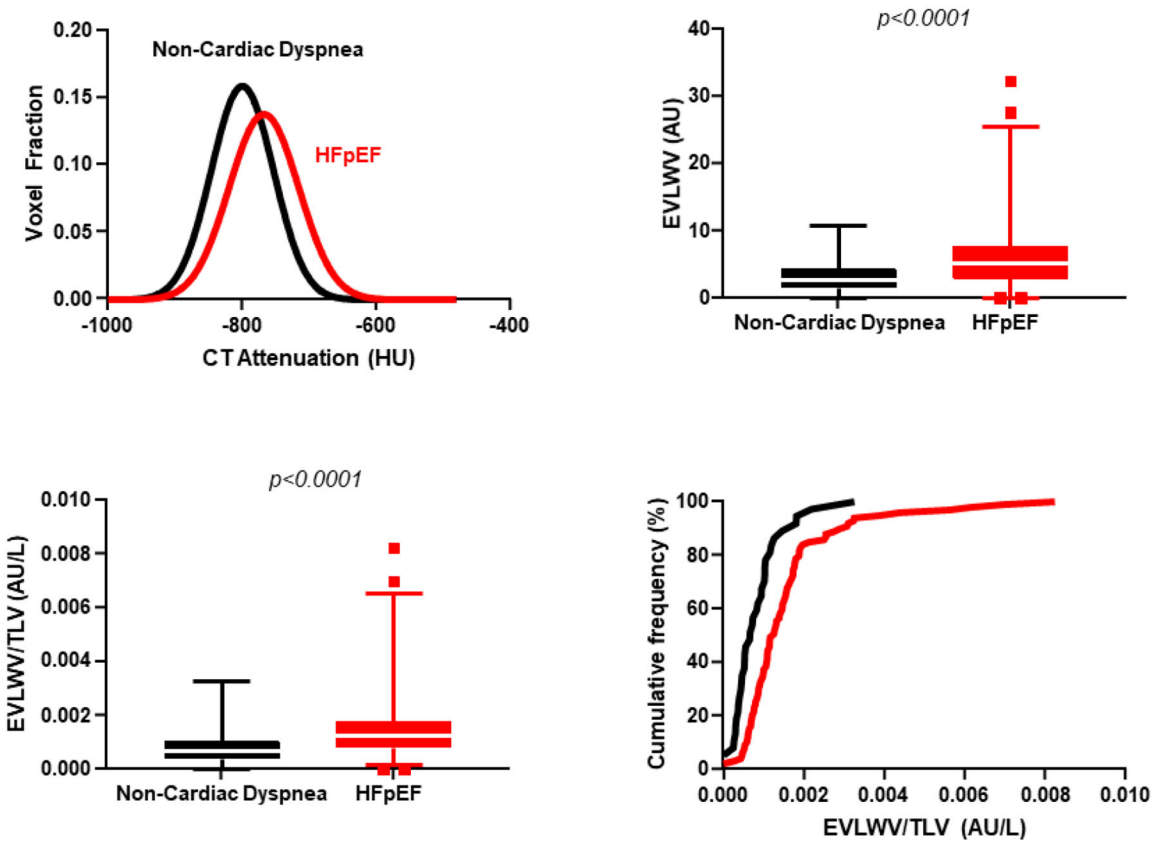

Central Illustration: Quantitative CT Analysis for Lung Congestion

The top left figure displays the distribution of mean lung density for controls (black) and for patients with HFpEF (red). The rightward shift, shorter peak, and wider curve are consistent with increased mean lung density and increased extravascular lung water in patients with HFpEF. Patients with HFpEF also displayed higher extravascular lung water volume (EVLWV, top right) and EVLWV/TLV (bottom left). Cumulative frequency distribution shows higher extravascular lung water as indicated by EVLWV to total lung volume (TLV) ratio in those with HFpEF (bottom right).

Abbreviations: AU = arbitrary units; CT = computed tomography; EVLWV = extravascular lung water volume; EVLWV/TLV = extravascular lung water volume indexed to total lung volume; HFpEF = heart failure with preserved ejection fraction; HU = Hounsfield units

Table 1:

Baseline Characteristics

	Non-cardiac dyspnea (n=38)	HFpEF (n=99)	p value
Demographics			
Age, years	58.4±14.9	68.0±12.2	0.0002
Female, n (%)	22 (58)	46 (46)	0.23
BMI, kg/m^2	25 (23, 28)	33 (28, 38)	<0.0001
Comorbidities, n (%)			
Hypertension	15 (39)	71 (71)	0.0007
Coronary Artery Disease	5 (23)	23 (37)	0.29
Atrial fibrillation, persistent	0 (0)	17 (18)	0.003
Diabetes mellitus	0 (0)	22 (22)	0.0005
Medications, n (%)			
Diuretics	6 (16)	58 (59)	<0.0001
ACEi/ARB	7 (18)	44 (44)	0.006
Beta blocker	8 (21)	57 (58)	0.0001
Laboratories			
Creatinine, mg/dL	1.0±0.3	1.1±0.4	0.09
Hemoglobin, g/dL	13.6±1.3	13.2±1.8	0.19
NT-ProBNP, pg/mL	64 (41, 199)	282 (71, 877)	0.0002
Echocardiography			
LVMI, g/m2	79.1±18.6	89.7±21.2	0.01
LAVI, ml/m^2	29±8	35±14	0.04
e' Septal, cm/s	8±2	7±2	0.005
E/e' Septal	8.9±3.4	13.3±6.6	0.0004
RVSP, mmHg	30±6	41±15	0.0001
Catheterization at Rest			
RAP, mmHg	6±3	12±5	<0.0001
PCWP, mmHg	13±4	19±5	<0.0001
PCWP V wave, mmHg	11±4	24±10	<0.0001
PA Systolic, mmHg	26±6	44±14	<0.0001
PA Diastolic, mmHg	9±4	20±7	<0.0001
PA Mean, mmHg	16±3	30±9	<0.0001
PA Compliance, ml/mmHg	4.5 (3.2, 6.0)	3.0 (2.0, 4.4)	<0.0001
PA Elastance, mmHg/ml	0.3 (0.3, 0.4)	0.6 (0.5. 0.8)	<0.0001
CI, L/m/m^2	2.8±0.6	2.4±0.6	0.006
PVR, WU	1.4 (1.2, 2.1)	2.4 (1.6, 3.4)	0.0005
Catheterization at Peak Exercise			
RAP, mmHg	9±3	22±8	<0.0001
PCWP, mmHg	16±4	33±7	<0.0001
PCWP V wave, mmHg	19±6	44±15	<0.0001
PA Systolic, mmHg	42±9	68±17	<0.0001

	Non-cardiac dyspnea (n=38)	**HFpEF (n=99)**	**p value**
PA Diastolic, mmHg	17±6	31±9	<0.0001
PA Mean, mmHg	27±6	48±11	<0.0001
PA Compliance, ml/mmHg	3.6 (2.8, 4.5)	2.6 (1.6, 3.9)	0.0002
PA Elastance, mmHg/ml	0.5 (0.4, 0.6)	0.7 (0.5, 1.2)	<0.0001
CI, L/m/m^2	5.6±1.5	4.2±1.6	0.002
PVR, WU	1.3 (1.0, 1.5)	1.9 (0.9, 2.9)	0.008

Abbreviations: ACEi/ARB = angiotensin converting enzyme inhibitor / angiotensin receptor blocker; BMI = body mass index; CI = cardiac index; LAVI = left atrial volume index; LVMI = left ventricular mass index; PA = pulmonary artery; PCWP = pulmonary capillary wedge pressure; PVR = pulmonary vascular resistance; RAP = right atrial pressure; RVSP = right ventricular systolic pressure

Table 2:

Lung Congestion by Quantitative Computed Tomography

	Non-cardiac dyspnea (n=38)	HFpEF (n=99)	p value
TLV (L)	4.1±1.8	4.1±1.7	0.99
Blood Volume (AU)	5.2 (2.98, 7.41)	8.5 (5.13, 12.4)	0.0003
Vessel Volume (AU)	127.6±66.1	116.1±57.4	0.32
EVLWV (AU)	2.7 (1.5, 4.3)	5.2 (2.9, 7.8)	<0.0001
EVLWV/TLV	0.66 (0.01, 1.03)	1.25 (0.80, 1.76)	<0.0001
Mean Lung Density (HU)	−787 (−828, −747)	−758 (−194, −708)	0.002
Skew	3.6 (3.0, 4.0)	2.9 (2.5, 3.3)	<0.0001
Kurtosis	15.2 (11.3, 20.0)	10.1 (7.27, 13.2)	<0.0001

Abbreviations: AU = arbitrary units; EVLWV = extravascular lung water volume; EVLWV/TLV = extravascular lung water volume indexed to total lung volume; HU = Hounsfield units; TLV = total lung volume

Table 3:

Correlations between Log (EVLWV/TLV) and Invasive Hemodynamics

	r	p value
Rest		
RAP	0.23	0.009
PCWP	0.25	0.004
PCWP V wave	0.30	0.0005
PA Systolic	0.35	<0.0001
PA Mean	0.35	<0.0001
PA Compliance	−0.17	0.06
PA Elastance	0.22	0.01
PVR	0.17	0.06
CI	−0.10	0.26
Peak		
RAP	0.32	0.0007
PCWP	0.32	0.0002
PCWP V wave	0.33	0.0002
PA Systolic	0.44	<0.0001
PA Mean	0.53	<0.0001
PA Compliance	−0.39	<0.0001
PA Elastance	0.38	<0.0001
PVR	0.31	0.0008
CI	−0.30	0.002

Abbreviations: CI = cardiac index; EVLWV/TLV = extravascular lung water volume indexed to total lung volume; PA = pulmonary artery; PCWP = pulmonary capillary wedge pressure; PVR = pulmonary vascular resistance; RAP = right atrial pressure